Nov 11th

# Buckling Strength of Plates

Zu-long Sun

Eighth International Specialty Conference on Cold-Formed Steel Structures
St. Louis, Missouri, U.S.A., November 11-12, 1986

# BUCKLING STRENGTH OF PLATES

by Zu-long Sun*

## INTRODUCTION

The buckling strength of a plate with three edges simply supported and one edge free under uniformly distributed compression acting on two opposite sides simply supported has been determined by Timoshenko(5). The buckling strength of plates with the above boundary conditions under nonuniformly distributed compression has been studied by Biljaard(1) and Walker(6) and others, but in their works the data is not complete. At the same time there are a few experiments of thin-walled members dealing with this subject.

The purpose of this paper is to show that the buckling strength for plates with the above boundary conditions under nonuniformly distributed compression has been calculated as completely as possible and the useful results have been obtained from a number of tests.

We all know that it is impossible to determine the exact buckling strength of plates under the above mentioned nonuniformly distributed compression. Therefore, in this paper, the approximate buckling strength can be determined by means of the principle of the minimum of total potential energy. Because the boundary conditions are complex, the method of Ritz with Lagrange multipliers is used during the process of minimization. As a result, the chosen functions for the buckling surface of a plate as a whole will be made to satisfy all the boundary conditions.

For the purpose of the requirements of the engineering and the convenience of applying the load to a specimen in the test the cold-formed thin-walled channels and angles are used as specimens.

*Assoc. Prof., Jiangxi Polytechnic University, The People's Republic of China.

## THE METHOD OF RITZ WITH LAGRANGE MULTIPLIERS

The expression for the total potential energy of a buckled elastic plate is shown as follows:

$$\Pi = \frac{D}{2}\int_o^a\int_o^b\{[\frac{\partial^2 w}{\partial x^2}+\frac{\partial^2 w}{\partial y^2}]^2-2(1-\nu)[\frac{\partial^2 w}{\partial x^2}\bullet\frac{\partial^2 w}{\partial y^2}-(\frac{\partial^2 w}{\partial x\partial y})^2]\}dxdy-\frac{1}{2}\int_o^a\int_o^b N_x(\frac{\partial w}{\partial x})^2dxdy \qquad (1)$$

where a = one-half the length of a plate buckling wave; b = width of the plate;

D = flexural rigidity; w = buckled surface; and $\nu$ = poisson's ratio.

The boundary conditions on two opposite loaded edges at x = 0 and x = a which are considered to be simply supported edges are:

$$w = 0 \qquad (2)$$

$$\frac{\partial^2 w}{\partial x^2}+\nu\frac{\partial^2 w}{\partial y^2} = 0 \qquad (3)$$

The boundary conditions along the unloaded edges are as follows: One edge simply supported at y = 0

$$w = 0 \qquad (4)$$

$$\frac{\partial^2 w}{\partial y^2}+\nu\frac{\partial^2 w}{\partial x^2} = 0 \qquad (5)$$

One edge free at y = b

$$\frac{\partial^2 w}{\partial y^2}+\nu\frac{\partial^2 w}{\partial x^2} = 0 \qquad (6)$$

$$\frac{\partial^3 w}{\partial y^3}+(2-\nu)\frac{\partial^3 w}{\partial x^2\partial y} = 0 \qquad (7)$$

The expression for the buckled surface of a plate may be assumed as follows:

$$W = \sum_{i=1}^{n} A_i\phi_i(Y)\sin\frac{\pi x}{a} \qquad (8)$$

It is clear that the expression (8) can satisfy the boundary conditions on two loaded simply supported edges at x = 0 and x = a. By choosing the $\phi i$ (y), the boundary conditions on simply supported edge at y = 0 can be satisfied too, but the boundary conditions on free edge, at $y = b$, can not be satisfied. That is, the equation (6) and (7) are not satisfied. This difficulty can be overcome by using the method of Ritz with Lagrange multipliers. Furthermore, this method may make calculations simpler.

Substituting the expression (8) into the equations (6) and (7), we obtain the following general relationship:

$$[L]\ [A]^T = 0 \tag{9}$$

$$[M]\ [A]^T = 0 \tag{10}$$

where $[L] = [L_1\ L_2\ L_3 \ldots L_n]$ (11)

$$[M] = [M_1\ M_2\ M_3 \ldots M_n] \tag{12}$$

$$[A] = [A_1\ A_2\ A_3 \ldots A_n] \tag{13}$$

After the equations (9) and (10) are multiplied by Lagrange multipliers $\lambda_1$ and $\lambda_2$ respectively and added to the expression (1), we may obtain a modified expression $\pi *$ for the total potential energy of an elastic plate as follows:

$$\pi^* = \pi + \lambda_1 [L]\ [A]^T + \lambda_2 [M]\ [A]^T \tag{14}$$

$$\pi = [A]\ [W]\ [A]^T \tag{15}$$

where

$$[W] = \begin{bmatrix} W_{11} & W_{12} & W_{13} & \cdots & W_{1n} \\ W_{21} & W_{22} & W_{23} & \cdots & W_{2n} \\ \vdots & \vdots & \vdots & & \vdots \\ W_{n1} & W_{n2} & W_{n3} & & W_{nn} \end{bmatrix} \tag{16}$$

By means of the principle of minimum potential energy, the modified expression (14) of the total potential energy is differentiated with respect to each $A_i$ and the resulting expressions are equal to zero. The result is as follows:

$$\frac{\partial \pi^*}{\partial A_1} = 2\sum_{i=1}^{n} W_{1i} A_i + \lambda_1 L_1 + \lambda_2 M_1 = 0$$

$$\frac{\partial \pi^*}{\partial A_2} = 2\sum_{i=1}^{n} W_{2i} A_i + \lambda_1 L_2 + \lambda_2 M_2 = 0$$

$$\frac{\partial \pi^*}{\partial An} = 2\sum_{i=1}^{n} W_{ni} A_i + \lambda_1 L_n + \lambda_2 Mn = 0$$

The above linear simultaneous equations for $A_i$ can be expressed in the matrix form as follows:

$$2[W][A]^T+\lambda_1 [L]^T+\lambda_2 [M]^T = 0 \tag{17}$$

and differentiated with respect to $\lambda_1$ and $\lambda_2$. The result is as follows:

$$\frac{\partial \Pi^*}{\partial \lambda_1} = [L][A]^T = 0 \tag{18}$$

$$\frac{\partial \pi^*}{\partial \lambda_2} = [M][A]^T = 0 \tag{19}$$

Equations (18) and (19) are identified with equations (9) and (10). The equation (17) contains a system of n linear equations. Thus, the above summation of equations (17), (18) and (19) results in a system of n + 2 homogeneous linear equations, in which the unknown numbers $A_i$ (i = 1,2,3...n) and $\lambda_1$, $\lambda_2$ have the same quantity as equations we get above.

After the equation (17) is premultiplied by $[W]^{-1}$, we obtain the following equation:

$$2 [A]^T = -\lambda_1 [W]^{-1} [L]^T - \lambda_2 [W]^{-1}[M]^T \tag{20}$$

Substituting the equation (20) into equations (18) and (19) respectively, we obtain as follows:

$$\lambda_1[L] [W]^{-1} [L]^T + \lambda_2 [L] [W]^{-1} [M]^T = 0 \tag{21}$$

$$\lambda_1[M] [W]^{-1} [L]^T + \lambda_2 [M] [W]^{-1} [M]^T = 0 \tag{22}$$

Because $\lambda_1$ and $\lambda_2$ can not equal zero, only the determinant of its coefficients are equal to zero, i.e.:

$$\begin{vmatrix} [L][W]^{-1}[L]^T & [L][W]^{-1}[M]^T \\ [M][W]^{-1}[L]^T & [M][W]^{-1}[M]^T \end{vmatrix} = 0 \tag{23}$$

where $[W]^{-1}$ is an inverse matrix of the square matrix [W].

We use just the above derived expression (23) to calculate the approximately buckling strength of plates.

## ANALYSIS OF THEORETICAL RESULTS

For the plate, as shown in Fig. 1, an approximate solution is considered by assuming the buckled surface in the form as follows:

$$\phi_1(y) = \frac{y}{b}; \quad \phi_i(y) = 0, \qquad i = 2, 3, 4 \ldots n.$$

thus
$$W = A_1\left(\frac{y}{b}\right)\mathrm{Sin}\frac{\pi x}{a} \tag{24}$$

where $A_1$ is a parameter, this form satisfies three edges simply supported and the geometric conditions along the free edge, but does not satisfy the expressions (6) and (7) of the forced boundary conditions.

Substituting the equation (24) into the equation (1) and performing the integration, the buckling stress of the plates under different nonuniformly distributed compressions is obtained as follows:

$$\sigma'_{cr} = \frac{N'cr}{t} = K'\frac{\pi^2 E}{12(1-\nu^2)}\left(\frac{t}{b}\right)^2$$

$$\text{or} \quad \sigma_{cr} = \frac{Ncr}{t} = K\frac{\pi^2 E}{12(1-\nu^2)}\left(\frac{t}{b}\right)^2 \tag{25}$$

where t = thickness of the plate; $K'(K)$ = buckling coefficient of the plate and $N'_{cr}(N_{cr})$ = critical compression

The critical compression "$N'_{cr}$" is applied to and parallel to the unloaded edge simply supported, the buckling coefficient of the plate, as shown in Fig. 1a is as follows:

$$K' = \left[0.425 + \left(\frac{b}{a}\right)^2\right]\frac{4}{4-3\alpha'} \tag{26}$$

where $\alpha' = (N'_{cr} - N'_o)/N'_{cr}$ ; $N'_o$ = compression (or tension) acting on and parallel to the unload free edge.

The critical compression "$N_{cr}$" is applied to and parallel to the unload free edge, as shown in Fig. 1b, the buckling coefficient of a plate is as follows:

$$K = \left[0.425 + \left(\frac{b}{a}\right)^2\right]\frac{4}{4-\alpha} \tag{27}$$

where $\alpha = (N_{cr} - N_o)/N_{cr}$

By calculating the flexural-torsional buckling strength of the single angle of equal legs under eccentric axial load acting in the symmetrical plane, the buckling coefficient can also be obtained as follows [2]:

$$K' = [0.425 + (1-\nu^2)\,(\frac{b}{a})^2]\,\frac{4}{4-3\alpha'} \tag{28}$$

$$K = [0.425 + (\,1-\nu^2)(\frac{b}{a})^2]\,\frac{4}{4-\alpha} \tag{29}$$

The above results are obtained by assuming that junction of the angle legs does not have transversal deflection.

It will be seen from contracting equations (26) and (27) to equations (28) and (29) that the expression (24) coincides with the assumption for the theory of flexural-torsional buckling of the open thin-walled section. It is noticed that if we take $\alpha' \to \frac{4}{3}$, by means of the equation (26) or (28), the buckling coefficient can be obtained as follows: $K' \to \infty$

The result implies that the buckling of the plate does not occur and that when eccentric load with sufficiently large negative eccentricity, shown in Fig. 2c and Fig. 2d, is applied to the symmetric plane of an angle of equal legs or a channel, the local buckling no longer occurs on a single angle or a channel with any slenderness ratios. This is impossible. In order to obtain the buckling strength of plates with three edges simply supported and one edge free under various compression nonuniformly distributed the buckled surface must be assumed as follows:

$$W = [A_1(\frac{y}{b})+A_2(\frac{y}{b})^3 + \sum_{i=1}^{4} A_{i+2}\mathrm{Sin}\,\frac{i\pi y}{b}]\mathrm{Sin}\,\frac{\pi x}{a} \tag{30}$$

After the substitution of the expression (30) in equations (9), (10) and (1) and after the integration of the elements of various matrices [L], [M] and [W] can be obtained and given in the Appendix III. The latter is substituted into the determinant (23). Eventually, the minimum buckling coefficients of the plate with three edges simply supported and one free edge under various compressions nonuniformly distributed may be obtained and are given in the Table 1.

It is found in the calculating process that a good approximation of buckling coefficients "K" is related to the expression (30) as follows:

1. When $0 \leq \alpha \leq 2.0$ and $\alpha' \leq 1.2$, in the calculation, only the expression of buckled surface (24) is taken, consequently, the buckling coefficients are obtained, that is, the expressions (26) and (27) are fairly exact.

2. When $\alpha' > 1.2$, only if the expression (30) is taken can we obtain a satisfactory approximate buckling coefficient given in the Table 1. It is interesting to note that these buckling coefficients ($\alpha' > 1.2$) are identical with the buckling coefficient of the plate with four edges simply supported under the same nonuniformly distributed compression. The above results have been checked by using the finite-difference method. The conclusion, as above mentioned, is quite correct. These results have also been confirmed from the buckling characteristic of a single angle in the experiment. Thus the choice of the expression (30) of the buckled surface is reasonable. It follows that the calculated buckling coefficients are reliable.

## EXPERIMENTAL INVESTIGATION

In order to examine the above theoretically calculated results about 50 specimens have been tested. In order to take account of the requirements on the practical engineering and the loaded convenience the cold-formed thin-walled channel and single angle are adopted as the specimens, as shown in Fig. 3. The overall nominal sizes of the specimens are exactly measured and are also listed in Table 2, 3, 4 and 5.

Eccentric load is applied to both ends of the specimens welded by end plates shown in Fig. 4. The eccentric axial load acting in the symmetric plane of the channel and angle makes the flanges (or legs) of a channel (or single angle) produce nonuniformly distributed compression. Moreover, the web-flange junction of the channel is considered as a simply supported edge, that coincides with the assumption which is made in the design. Practically, the two junctions are elastically restricted to each other. Experimental buckling coefficients were obtained by the strain reversal method [7]. Experimental details are given in Ref. 4.

The geometrical characteristics of the specimens of channels and angles, experimental results, buckling compressions and so on all are listed in Tables 2, 3, 4 and 5.

## ANALYSIS OF TEST RESULTS

CHANNELS

1. It is found in Tables 2 and 3 that the buckling coefficients "K" or "K'" are calculated according to the expressions (26) and (27). When $0 \leq \alpha \leq 2.0$ and $\alpha' \leq 1.2$, it can meet the requirements of the design. If $\alpha' > 1.2$, the total buckling deformation occurs at two flanges near the web-flange junctions shown in Fig. 5a, but the free edge of the flanges has only a little deflection. It can be seen from this that the buckling characteristic is the same as the buckling deflection of the plate with four edges simply supported. The effect of initial imperfections on the buckling strength is of less importance because of the elastic restraints acting on web-flange junction.

2. With the increase of the tensile stress in the web, the effect of the elastic restraints on the flanges decreases. On the contrary, with the increase of the compressive stress in the web, the effect of the elastic restraints on the flanges increases. Therefore, when an unstiffened channel is subjected by a compression with small eccentricity, its flange checked by means of the buckling coefficients listed in Table 1 is conservative.

SINGLE ANGLE

1. We have tested two specimens of which $\alpha' = 1.5$, the experimental results have shown that the local buckling of the individual legs lead in the overall collapse of the angle. At the same time we may see a concave at the middle region of one leg near the junction of legs and a convex at the same place of the other leg, as

shown in Fig. 5b the deflection at the middle span of the free edge is very small. The buckling and deflecting characteristics as mentioned above, are identical with those of the plate with four edges simply supported under the same load. This phenomena also demonstrates that the theoretical calculation in this paper is correct.

2. We also tested various eccentricities at the symmetric plane of thin-walled single angles of the equal legs, the flexural-torsional buckling occurs on many of the angles and the buckling strength is less than the value of the theoretical calculation, as shown in Tables 4 and 5.

## CONCLUSION

The buckling coefficients "K" or "K'" of the plate with three edges simply supported and one edge free, as shown in Table 1, can be used to calculate the local buckling of the flange of a unstiffened channel under nonuniformly distributed compression.

When the buckling coefficients "K" or "K'" of the plate, as shown in Table 1, are used to calculate the local buckling strength of a leg of angles, in order to take account of the unfavorable effect of initial imperfections on it, the buckling coefficients in Table 1 should be a little smaller.

## APPENDIX I REFERENCES

1. Biljaard, P.P., "Buckling of Plate Under Non-Homogeneous Stress", Journal of the Engineering Mechanics Division, ASCE Proceeding, vol. 83, No. EM3, July 1957, p. 1293.

2. Bleich, F., Buckling Strength of Metal Structures, New York, 1952.

3. McFarland, D., Smith, B.L., and Bernhart, W.D., Analysis of Plates, New York, 1972.

4. Sun, Z.L. and He, H.X., "Investigation of Experiment and Calculation for Buckling Strength of the Rectangular Plate With Three Edges Simply Supported and One Edge Free Under Nonuniform Compression", selections from research paper and reports on steel structures, vol. 1, China Technical Committee for Standards of Steel Structures, 1982.

5. Timoshenko, S.P., and Gere, J.M., Theory of Elastic Stability, 2nd Edition, New York, 1961.

6. Walker, A.C., "Local Instability in Plates and Channel Struts", Journal of the Structural Division, ASCE Proceedings, vol. 92, no. ST3, June 1966, pp. 39-55.

7. Vann, W.P. and Sehested, J., "Experimental Techniques for Plate Buckling", Proceedings of the Second Specialty Conference on Cold-Formed Steel Structures, St. Louis, MO, October 1973, pp. 83-105.

## APPENDIX II NOTATION

The following symbols are used in this paper:

$A_i$ = coefficient in deflection series;

a = one-half the length of the buckling wave of plate;

b = width of plate;

c = centroid;

D = flexural rigidity of plate;

E = modulus of elasticity;

h = width of web plate of channel;

K(or K') = buckling coefficient of plate;

l = length of specimen;

$N_{cr}$(or $N'_{cr}$) = critical compression;

$P_{cr}$ = theoretical eccentric buckling load on specimen;

$P^t_{cr}$ = eccentric buckling load on specimen derived from test;

$P^t_u$ = eccentric load at failure for testing specimen;

t = thickness of plate;

W = buckled surface of plate;

$\alpha$(or $\alpha'$) = eccentric coefficient = $\frac{N_{cr} - N_o}{N_{cr}}$ (or $\alpha' = \frac{N'_{cr} - N'_o}{N'_{cr}}$);

$\lambda$ = parameter in analysis;

$\lambda_1$, $\lambda_2$ = Lagrange multiplier;

$\nu$ = Poisson's ratio;

$\sigma_{cr}$ $= \frac{N_{cr}}{t} = K \frac{\pi^2 E}{12(1 - \nu^2)} (\frac{t}{b})^2$;

$\sigma'_{cr}$ $= \frac{N'_{cr}}{t} = K' \frac{\pi^2 E}{12(1 - \nu^2)} (\frac{t}{b})^2$;

$\Psi$ = parameter in analysis.

## APPENDIX III

THE ELEMENTS OF THE VARIOUS MATRICES [L], [M] AND [W]

$$L_1 = -0.3\pi^2 \left(\frac{b}{a}\right)^2$$

$$L_2 = 6-0.3\pi^2\left(\frac{b}{a}\right)^2$$

$$L_3 = L_4 = L_5 = L_6 = 0$$

$$M_1 = -1.7\pi^2\left(\frac{b}{a}\right)^2$$

$$M_2 = 6-5.1\pi^2\left(\frac{b}{a}\right)^2$$

$$M_3 = \pi^3\left[1+1.7\left(\frac{b}{a}\right)^2\right]$$

$$M_4 = -2\pi^3\left[4+1.7\left(\frac{b}{a}\right)^2\right]$$

$$M_5 = 3\pi^3\left[9+1.7\left(\frac{b}{a}\right)^2\right]$$

$$M_6 = -4\pi^3\left[16+1.7\left(\frac{b}{a}\right)^2\right]$$

$$W_{11} = \frac{a}{2b}\left(\frac{\pi}{a}\right)^2\left\{\frac{D}{2}\left[1.4+\frac{1}{3}\left(\frac{\pi b}{\alpha}\right)^2\right]-Ncr\,\frac{b^2}{2}\left(\frac{\Psi}{3}-\frac{\lambda}{4}\right)\right\}$$

$$W_{12} = W_{21} = \frac{a}{2b}\left(\frac{\pi}{a}\right)^2\left\{\frac{D}{2}\left[0.8+\frac{1}{5}\left(\frac{\pi b}{a}\right)^2\right]-Ncr\,\frac{b^2}{2}\left(\frac{\Psi}{5}+\frac{\lambda}{6}\right)\right\}$$

$$W_{13} = W_{31} = \frac{a}{2b}\left(\frac{\pi}{a}\right)^2\left\{\frac{D}{2}\pi\left[0.3+\left(\frac{b}{a}\right)^2\right]-Ncr\,\frac{b^2}{2\pi}\left[\Psi+\lambda\left(1-\frac{4}{\pi^2}\right)\right]\right\}$$

$$W_{14} = W_{41} = \frac{a}{2b}\left(\frac{\pi}{a}\right)^2\left\{\frac{D}{2}\pi\left[-0.6-\frac{1}{2}\left(\frac{b}{a}\right)^2\right]+Ncr\,\frac{b^2}{2}\,\frac{1}{2\pi}(\Psi+\lambda)\right\}$$

$$W_{15} = W_{51} = \frac{a}{2b}\left(\frac{\pi}{a}\right)^2\left\{\frac{D}{2}3\pi\left[0.3+\frac{1}{9}\left(\frac{b}{a}\right)^2\right]-Ncr\,\frac{b^2}{2}\,\frac{1}{3\pi}\left[\Psi+\lambda\left(1-\frac{4}{9\pi^2}\right)\right]\right\}$$

$$W_{16} = W_{61} = \frac{a}{2b}\left(\frac{\pi}{a}\right)^2\left\{\frac{D}{2}4\pi\left[-0.3-\frac{1}{16}\left(\frac{b}{a}\right)^2\right]+Ncr\,\frac{b^2}{2}\,\frac{1}{4\pi}(\Psi+\lambda)\right\}$$

$$W_{22} = \frac{a}{2b}\left(\frac{\pi}{a}\right)^2\left\{\frac{D}{2}\left[12\left(\frac{a}{\pi b}\right)^2+\frac{9}{5}+\frac{1}{7}\left(\frac{\pi b}{a}\right)^2\right]-Ncr\,\frac{b^2}{2}\left(\frac{\Psi}{7}+\frac{\lambda}{8}\right)\right\}$$

$$W_{23} = W_{32} = \frac{a}{2b}\left(\frac{\pi}{a}\right)^2\left\{\frac{D}{2}\left[\pi\left(0.3+\frac{b^2}{a^2}\right)-\frac{6}{\pi}\left(\frac{a}{b}+\frac{b}{a}\right)^2\right]-Ncr\,\frac{b^2}{2}\,\frac{1}{\pi}\left[\Psi\left(1-\frac{6}{\pi^2}\right)+\lambda\left(1-\frac{12}{\pi^2}+\frac{48}{\pi^4}\right)\right]\right\}$$

$$W_{24} = W_{42} = \frac{a}{2b}\left(\frac{\pi}{a}\right)^2\left\{\frac{D}{2}\,\frac{3}{\pi}\left(\frac{2a}{b}+\frac{b}{2a}\right)^2-2\pi\left(0.3+\frac{b^2}{4a^2}\right)\right]+Ncr\,\frac{b^2}{2}\,\frac{1}{2\pi}\left[\Psi\left(1-\frac{3}{2\pi^2}\right)+\lambda\left(1-\frac{3}{\pi^2}\right)\right]\right\}$$

$$W_{25} = W_{52} = \frac{a}{2b}\left(\frac{\pi}{a}\right)^2\left\{\frac{D}{2}\left[3\pi\left(0.3+\frac{b^2}{9a^2}\right)-\frac{2}{\pi}\left(\frac{3a}{b}+\frac{b}{3a}\right)^2\right]\right.$$

$$\left.-Ncr\,\frac{b^2}{2}\,\frac{1}{3\pi}\left[\Psi\left(1-\frac{2}{3\pi^2}\right)+\lambda\left(1-\frac{4}{3\pi^2}+\frac{16}{27\pi^4}\right)\right]\right\}$$

$$W_{26} = W_{62} = \frac{a}{2b}\left(\frac{\pi}{a}\right)^2 \{\frac{D}{2}[\frac{3}{2\pi}\left(\frac{4a}{b}+\frac{b}{4a}\right)^2 - 4\pi\,(0.3 + \frac{b^2}{16a^2})]$$

$$+ Ncr\,\frac{b^2}{2}\,\frac{1}{4\pi}\,[\Psi(1 - \frac{3}{8\pi^2}) + \lambda(1 - \frac{3}{4\pi^2})]\}$$

$$W_{33} = \frac{a}{2b}\left(\frac{\pi}{a}\right)^2 \{\frac{D}{2}\,\frac{\pi^2}{2}\left(\frac{a}{b} + \frac{b}{a}\right)^2 - Ncr\,\frac{b^2}{2}\,\frac{1}{2}\,(\Psi + \frac{\lambda}{2})\}$$

$$W_{34} = W_{43} = \frac{a}{2b}\left(\frac{\pi}{a}\right)^2 Ncr\,\frac{b^2}{2}\lambda\,\frac{8}{9\pi^2}$$

$$W_{35} = W_{53} = 0$$

$$W_{36} = W_{63} = \frac{a}{2b}\left(\frac{\pi}{a}\right)^2 Ncr\,\frac{b^2}{2}\,\lambda\left(\frac{4}{15\pi}\right)^2$$

$$W_{44} = \frac{a}{2b}\left(\frac{\pi}{a}\right)^2 \{\frac{D}{2}\,\frac{\pi^2}{2}\left(\frac{4a}{b} + \frac{b}{a}\right)^2 - Ncr\,\frac{b^2}{2}\,\frac{1}{2}\,(\Psi + \frac{\lambda}{2})\}$$

$$W_{45} = W_{54} = \frac{a}{2b}\left(\frac{\pi}{a}\right)^2 Ncr\,\frac{b^2}{2}\,\lambda\,\frac{24}{25\pi^2}$$

$$W_{46} = W_{64} = 0$$

$$W_{55} = \frac{a}{2b}\left(\frac{\pi}{a}\right)^2 \{\frac{D}{2}\,\frac{\pi^2}{2}\left(\frac{9a}{b} + \frac{b}{a}\right)^2 - Ncr\,\frac{b^2}{2}\,\frac{1}{2}\,(\Psi + \frac{\lambda}{2})\}$$

$$W_{56} = W_{65} = \frac{a}{2b}\left(\frac{\pi}{a}\right)^2 Ncr\,\frac{b^2}{2}\,\lambda\,\frac{48}{49\pi^2}$$

$$W_{66} = \frac{a}{2b}\left(\frac{\pi}{a}\right)^2 \{\frac{D}{2}\,\frac{\pi^2}{2}\left(\frac{16a}{b} + \frac{b}{a}\right)^2 - Ncr\,\frac{b^2}{2}\,\frac{1}{2}\,(\Psi + \frac{\lambda}{2})\}$$

Notes: $\Psi$ and $\lambda$ = parameters in analysis.

1. For determining buckling coefficients K, $\Psi = 1-\alpha$ and $\lambda = \alpha$.
2. For determining buckling coefficients K', $\Psi = 1$ and $\lambda = -\alpha'$.

TABLE 1

Buckling Coefficients Determined According To Eg. (23)

| | a/b | | 1 | 10 | 100 | 1000 |
|---|---|---|---|---|---|---|
| α | 0.0 | K | 1.425 | 0.435 | 0.425 | 0.425 |
| | 0.4 | | 1.583 | 0.483 | 0.472 | 0.472 |
| | 1.0 | | 1.9 | 0.58 | 0.567 | 0.567 |
| | 2.0 | | 2.85 | 0.87 | 0.85 | 0.85 |
| α' | 0.0 | K' | 1.425 | 0.435 | 0.425 | 0.425 |
| | 0.4 | | 2.036 | 0.620 | 0.607 | 0.607 |
| | 1.0 | | 4.80 (5.70) | 1.74 | 1.70 | 1.70 |
| | 1.2 | | 7.30 (14.25) | 4.31 | 4.251 | 4.25 |

| | a/b | | 0.35 | 0.4 | 0.6 | 0.667 | 0.8 | 1.0 | 1.3 | 1.5 |
|---|---|---|---|---|---|---|---|---|---|---|
| α' | 1.33 | K' | | | 10.8 | 10.5 | 10.1 | 9.7 | 9.4 | 9.4 |
| | 1.6 | | | | 15.2 | 15.1 | 15.0 | 15.3 | 15.9 | |
| | 1.8 | | | 19.7 | 19.2 | 19.3 | 19.6 | 20.3 | 21.9 | 23.0 |
| | 2.0 | | 24.1 | 23.9 | 24.2 | 24.6 | 25.5 | 26.9 | 29.6 | 31.5 |

Note: Values given in brackets are determined according to Eg. (26).

TABLE 2

Geometrical characteristics, theoretical and experimental results of specimens made of channels subjected to eccentric loads $P_{cr}^{t}$ and $P_{u}^{t}$ with eccentric coefficient $\alpha = \frac{Ncr - No}{Ncr}$

| speci-men | $\alpha$ | h (in) | b (in) | t (in) | l (in) | $\delta o$ (in) | $\frac{\delta o}{b}$ | $P_{cr}$ (kips) | $P_{cr}^{t}$ (kips) | $P_{u}^{t}$ (kips) | $\frac{P_{cr}^{t}}{P_{cr}}$ | $\frac{P_{u}^{t}}{P_{u}}$ |
|---|---|---|---|---|---|---|---|---|---|---|---|---|
| CA1 | 0.2 | 3.9 | 2.4 | 0.1 | 23.6 | 0.0012 | $\frac{1}{2000}$ | 13.78 | ------ | 16.98 | ------ | 1.24 |
| CA2 | 0.2 | 3.9 | 2.4 | 0.1 | 23.6 | 0.012 | $\frac{1}{200}$ | ----- | ------ | 19.29 | ------ | 1.40 |
| CA3 | 0.2 | 3.9 | 2.4 | 0.1 | 23.6 | 0.032 | $\frac{1}{73}$ | 13.78 | 14.33 | 16.65 | 1.04 | 1.21 |
| $CB_1$ | 0.2 | 4.7 | 3.1 | 0.1 | 31.5 | 0.011 | $\frac{1}{276}$ | 9.83 | 14.33 | 21.17 | 1.45 | 2.17 |
| $CB_2$ | 0.2 | 4.7 | 3.1 | 0.1 | 31.5 | 0.038 | $\frac{1}{82}$ | 9.83 | 14.33 | 19.85 | 1.45 | 2.02 |
| $CC_1$ | 0.2 | 5.9 | 3.9 | 0.1 | 39.4 | ----- | ---- | 7.84 | 14.99 | 18.52 | 1.91 | 2.36 |
| $CD_1$ | 0.2 | 7.1 | 4.1 | 0.1 | 39.4 | 0.017 | $\frac{1}{233}$ | 8.00 | 9.92 | 14.33 | 1.24 | 1.79 |
| $CA_4$ | 0.4 | 3.9 | 2.4 | 0.1 | 23.6 | 0.019 | $\frac{1}{125}$ | 11.91 | 13.23 | 14.88 | 1.11 | 1.25 |
| $CA_5$ | 0.4 | 3.9 | 2.4 | 0.1 | 23.6 | 0.007 | $\frac{1}{316}$ | 11.91 | 13.23 | 14.88 | 1.11 | 1.25 |
| $CA_6$ | 0.4 | 3.9 | 2.4 | 0.1 | 23.6 | 0.014 | $\frac{1}{167}$ | 11.91 | ------ | 16.98 | ------ | 1.43 |
| $CA_7$ | 0.4 | 3.9 | 2.4 | 0.1 | 23.6 | 0.01 | $\frac{1}{231}$ | 11.91 | ------ | 18.30 | ------ | 1.54 |
| $CA_8$ | 0.4 | 3.9 | 2.4 | 0.1 | 23.6 | 0.003 | $\frac{1}{750}$ | 11.91 | ------ | 15.10 | ------ | 1.27 |
| $CB_3$ | 0.8 | 4.7 | 3.1 | 0.1 | 31.5 | 0.017 | $\frac{1}{182}$ | 5.93 | 8.82 | 11.25 | 1.49 | 1.90 |

(Continued)

TABLE 2

Geometrical characteristics, theoretical and experimental results of specimens made of channels subjected to eccentric loads $P_{cr}^{t}$ and $P_{u}^{t}$ with eccentric coefficient $\alpha = \frac{Ncr - No}{Ncr}$

| specimen | $\alpha$ | h (in) | b (in) | t (in) | l (in) | $\delta o$ (in) | $\frac{\delta o}{b}$ | $P_{cr}$ (kips) | $P_{cr}^{t}$ (kips) | $P_{u}^{t}$ (kips) | $\frac{P_{cr}^{t}}{P_{cr}}$ | $\frac{P_{u}^{t}}{P_{cr}}$ |
|---|---|---|---|---|---|---|---|---|---|---|---|---|
| $CB_4$ | 0.8 | 4.7 | 3.1 | 0.1 | 31.5 | 0.002 | $\frac{1}{1600}$ | 5.93 | 8.82 | 11.25 | 1.49 | 1.90 |
| $CB_5$ | 0.8 | 4.7 | 3.1 | 0.1 | 31.5 | ----- | ---- | 5.93 | 8.82 | 9.32 | 1.49 | 1.57 |
| $CB_6$ | 0.8 | 4.7 | 3.1 | 0.1 | 31.5 | 0.013 | $\frac{1}{41}$ | 5.93 | 6.84 | 8.16 | 1.15 | 1.38 |
| $CA_9$ | 1.0 | 3.9 | 2.4 | 0.1 | 23.6 | 0.004 | $\frac{1}{100}$ | 5.84 | 8.6 | 9.48 | 1.47 | 1.62 |
| $CA_{10}$ | 1.0 | 3.9 | 2.4 | 0.1 | 23.6 | 0.034 | $\frac{1}{70}$ | 5.84 | ---- | 9.37 | ---- | 1.60 |
| $CC_2$ | 1.0 | 5.9 | 3.9 | 0.1 | 39.4 | 0.016 | $\frac{1}{250}$ | 3.51 | 4.63 | 6.84 | 1.32 | 1.95 |
| $CC_3$ | 1.0 | 5.9 | 3.9 | 0.1 | 39.4 | 0.025 | $\frac{1}{159}$ | 3.51 | 5.51 | 8.05 | 1.57 | 2.30 |
| $CC_4$ | 1.6 | 5.9 | 3.9 | 0.1 | 39.4 | 0.01 | $\frac{1}{400}$ | -2.25* | -6.84 | 10.58 | 3.04 | 4.70 |
| $CD_2$ | 1.6 | 7.1 | 4.1 | 0.1 | 39.4 | 0.012 | $\frac{1}{339}$ | -3.05* | -2.87 | -4.85 | 1.08 | 1.84 |
| $CD_3$ | 1.6 | 7.1 | 4.1 | 0.1 | 39.4 | 0.024 | $\frac{1}{169}$ | -3.05* | -3.31 | -5.07 | 1.25 | 1.92 |
| $CE_1$ | 2.0 | 5.9 | 5.9 | 0.1 | 47.2 | 0.051 | $\frac{1}{116}$ | -3.84* | -3.75 | -6.39 | 1.07 | 1.84 |
| $CE_2$ | 2.0 | 5.9 | 5.9 | 0.1 | 47.2 | 0.98 | $\frac{1}{153}$ | -3.48* | -3.75 | -6.39 | 1.07 | 1.84 |

* Tension

TABLE 3

Geometrical characteristics, theoretical and experimental results of specimens made of channels subjected to eccentric loads $P^t_{cr}$ and $P^t_u$ with eccentric coefficient $\alpha' = \frac{N'_{cr} - N'_o}{N'_{cr}}$

| speci-men | $\alpha'$ | h (in) | b (in) | t (in) | l (in) | $\delta o$ (in) | $\frac{\delta o}{b}$ | $P'_{cr}$ (kips) | $P'^t_{cr}$ (kips) | $P'^t_u$ (kips) | $\frac{P'^t_{cr}}{P'_{cr}}$ | $\frac{P'^t_u}{P'_{cr}}$ |
|---|---|---|---|---|---|---|---|---|---|---|---|---|
| $CB_7$ | 0.4 | 4.7 | 3.1 | 0.1 | 31.5 | 0.017 | $\frac{1}{182}$ | 13.97 | ---- | 26.4 | ---- | 1.89 |
| $CB_8$ | 0.4 | 4.7 | 3.1 | 0.1 | 31.5 | ----- | ---- | 13.97 | 19.8 | 24.2 | 1.41 | 1.73 |
| $CB_9$ | 0.4 | 4.7 | 3.1 | 0.1 | 31.5 | 0.056 | $\frac{1}{56}$ | 13.97 | 17.6 | 21.78 | 1.34 | 1.56 |
| $CB_{10}$ | 0.4 | 4.7 | 3.1 | 0.1 | 31.5 | 0.04 | $\frac{1}{78}$ | 13.97 | 13.2 | 18.66 | 0.95 | 1.33 |
| $CB_{11}$ | 0.6 | 4.7 | 3.1 | 0.1 | 31.5 | 0.02 | $\frac{1}{157}$ | 17.05 | ---- | 26.4 | ---- | 1.54 |
| $CB_{12}$ | 0.6 | 4.7 | 3.1 | 0.1 | 31.5 | 0.023 | $\frac{1}{136}$ | 17.05 | 19.8 | 24.2 | 1.16 | 1.42 |
| $CB_{13}$ | 0.6 | 4.7 | 3.1 | 0.1 | 31.5 | 0.011 | $\frac{1}{296}$ | 17.05 | 17.6 | 22.0 | 1.03 | 1.29 |
| $CB_{14}$ | 0.6 | 4.7 | 3.1 | 0.1 | 31.5 | 0.011 | $\frac{1}{196}$ | 17.05 | 17.6 | 23.1 | 1.03 | 1.35 |
| $CF_1$ | 1.0 | 5.9 | 4.7 | 0.1 | 39.4 | 0.017 | $\frac{1}{273}$ | 19.91 | ---- | 26.4 | ---- | 1.33 |
| $CF_2$ | 1.0 | 5.9 | 4.7 | 0.1 | 39.4 | 0.007 | $\frac{1}{706}$ | 19.91 | ---- | 25.96 | ---- | 1.30 |
| $CF_3$ | 1.0 | 5.9 | 4.7 | 0.1 | 39.4 | 0.008 | $\frac{1}{545}$ | 19.91 | ---- | 26.4 | ---- | 1.33 |
| $CG_1$ | 1.0 | 3.1 | 4.7 | 0.1 | 39.4 | 0.022 | $\frac{1}{218}$ | 14.76 | ---- | 25.52 | ---- | 1.73 |
| $CG_2$ | 1.0 | 3.1 | 4.7 | 0.1 | 39.4 | 0.041 | $\frac{1}{114}$ | 14.76 | ---- | 25.3 | ---- | 1.72 |

TABLE 4

Geometrical characteristics, theoretical and experimental results of specimens made of angels subjected to eccentric loads $P^t_{cr}$ and $P^t_u$ with eccentric coefficient $\alpha = \frac{Ncr - No}{Ncr}$

| speci-men | | b (in) | t (in) | l (in) | δo (in) | $\frac{\delta o}{b}$ | $P_{cr}$ (kips) | $P^t_{cr}$ (kips) | $P^t_u$ (kips) | $\frac{P^t_{cr}}{P_{cr}}$ | $\frac{P^t_u}{P_{cr}}$ |
|---|---|---|---|---|---|---|---|---|---|---|---|
| A15-1 | 0.6 | 5.9 | 0.11 | 23.6 | 0.019 | $\frac{1}{311}$ | 4.64 | 3.52 | 7.04 | 0.76 | 1.52 |
| A15-2 | 0.61 | 5.9 | 0.11 | 23.6 | 0.039 | $\frac{1}{151}$ | 4.61 | 3.96 | 6.60 | 0.86 | 1.43 |
| A15-3 | 0.735 | 5.9 | 0.11 | 23.6 | 0.030 | $\frac{1}{197}$ | 4.36 | 4.84 | 6.16 | 1.11 | 1.41 |
| A15-4 | 1.04 | 5.9 | 0.11 | 23.6 | ----- | --- | 3.63 | 3.30 | 5.81 | 0.91 | 1.60 |
| A15-5 | 1.36 | 5.9 | 0.11 | 23.6 | 0.039 | $\frac{1}{151}$ | 2.73 | 2.2 | 3.08 | 0.81 | 1.13 |
| A15-6 | 1.45 | 5.9 | 0.11 | 23.6 | 0.015 | $\frac{1}{393}$ | 2.44 | 2.2 | 2.99 | 0.91 | 1.23 |
| A15-7 | 1.48 | 5.9 | 0.11 | 23.6 | ----- | --- | 2.31 | 2.2 | 3.08 | 0.95 | 1.33 |
| A15-8 | 1.63 | 5.9 | 0.11 | 23.6 | 0.019 | $\frac{1}{311}$ | 1.76 | 1.76 | 3.08 | 1.00 | 1.75 |
| A12-1 | 0.00 | 4.7 | 0.11 | 23.6 | 0.019 | $\frac{1}{247}$ | 7.04 | 7.04 | 8.80 | 1.00 | 1.25 |
| A12-2 | 0.87 | 4.7 | 0.11 | 23.6 | 0.011 | $\frac{1}{427}$ | 5.06 | 3.52 | 5.68 | 0.70 | 1.12 |
| A12-3 | 1.00 | 4.7 | 0.11 | 23.6 | ----- | --- | 4.72 | 3.96 | 5.59 | 0.84 | 1.18 |
| A12-4 | 1.01 | 4.7 | 0.11 | 23.6 | 0.019 | $\frac{1}{247}$ | 4.68 | 3.52 | 4.62 | 0.75 | 0.99 |
| A12-5 | 1.42 | 4.7 | 0.11 | 23.6 | 0.006 | $\frac{1}{783}$ | 3.17 | 2.64 | 3.23 | 0.83 | 1.02 |
| A8-1 | 0.00 | 3.2 | 0.11 | 23.6 | 0.026 | $\frac{1}{123}$ | 10.56 | 9.46 | 10.12 | 0.90 | 0.96 |
| A8-2 | 0.22 | 3.2 | 0.11 | 23.6 | ----- | --- | 9.95 | 8.14 | 8.8 | 0.82 | 0.88 |
| A8-3 | 0.25 | 3.2 | 0.11 | 23.6 | 0.018 | $\frac{1}{178}$ | 9.79 | 8.36 | 8.98 | 0.85 | 0.92 |
| A8-4 | 1.12 | 3.2 | 0.11 | 23.6 | 0.009 | $\frac{1}{356}$ | 6.45 | 4.64 | 4.95 | 0.72 | 0.77 |
| A8-5 | 1.38 | 3.2 | 0.11 | 23.6 | 0.009 | $\frac{1}{365}$ | 5.01 | 3.96 | 4.18 | 0.79 | 0.83 |

TABLE 5

Geometrical characteristics, theoretical and experimental results of specimens made of angles subjected to eccentric loads $P_{cr}^{'t}$ and $P_{u}^{'t}$ with eccentric coefficient $\alpha' = \frac{Ncr - No}{N'cr}$

| speci-men | $\alpha'$ | b (in) | t (in) | l (in) | $\delta o$ (in) | $\frac{\delta o}{b}$ | $P'_{cr}$ (kips) | $P'^{t}_{u}$ (kips) | $P'^{t}_{cr}$ (kips) | $\frac{P'^{t}_{cr}}{P'_{cr}}$ | $\frac{P'^{t}_{u}}{P'_{cr}}$ |
|---|---|---|---|---|---|---|---|---|---|---|---|
| A15-9 | 0.62 | 5.9 | 0.11 | 23.6 | ----- | ---- | 7.22 | 6.6 | 9.9 | 0.91 | 1.37 |
| A15-10 | 0.63 | 5.9 | 0.11 | 23.6 | ----- | ---- | 7.35 | 6.6 | 8.8 | 9.90 | 1.20 |
| A15-11 | 0.65 | 5.9 | 0.11 | 23.6 | ----- | ---- | 7.43 | 6.6 | 10.12 | 0.89 | 1.36 |
| A15-12 | 1.05 | 5.9 | 0.11 | 23.6 | ----- | ---- | 12.59 | 14.08 | 16.94 | 1.12 | 1.35 |
| A15-13 | 1.14 | 5.9 | 0.11 | 23.6 | ----- | ---- | 16.7 | 15.84 | ---- | 0.95 | ----- |
| A12-6 | 0.18 | 4.7 | 0.11 | 23.6 | 0.02 | $\frac{1}{253}$ | 7.39 | 7.7 | 9.02 | 1.04 | 1.22 |
| A12-7 | 0.53 | 4.7 | 0.11 | 23.6 | ----- | ---- | 8.65 | 6.6 | 9.9 | 0.76 | 1.14 |
| A12-8 | 0.90 | 4.7 | 0.11 | 23.6 | 0.006 | $\frac{1}{783}$ | 11.84 | 8.8 | 14.74 | 0.74 | 1.24 |
| A12-9 | 0.94 | 4.7 | 0.11 | 23.6 | 0.019 | $\frac{1}{247}$ | 12.65 | 9.9 | 14.30 | 0.78 | 1.13 |
| A8-6 | 0.26 | 3.2 | 0.11 | 23.6 | 0.011 | $\frac{1}{291}$ | 11.46 | 9.9 | 10.45 | 0.86 | 0.91 |
| A8-7 | 0.35 | 3.2 | 0.11 | 23.6 | 0.007 | $\frac{1}{457}$ | 11.89 | 11.0 | 11.62 | 0.93 | 0.98 |

Notes:

1. Symbols used for dimensions are shown in Fig. 3
2. 1 inch = 25.4 mm; 1 kip = 4.45KN.
3. $\nu = 0.3$.
4. $E = 29.5\ 10^3$ Ksi $= 203.76\ 10^3$ mpa.
5. $l$ = length of specimen.
6. $\delta o$ = initial average deflection in the middle of two free edges of the specimen.
7. $P_{cr}$ = theoretical eccentric buckling load on specimen.
8. $P^t_{cr}$ = eccentric buckling load on specimens obtained from test.
9. $P^t_u$ = eccentric load at failure for testing specimens.

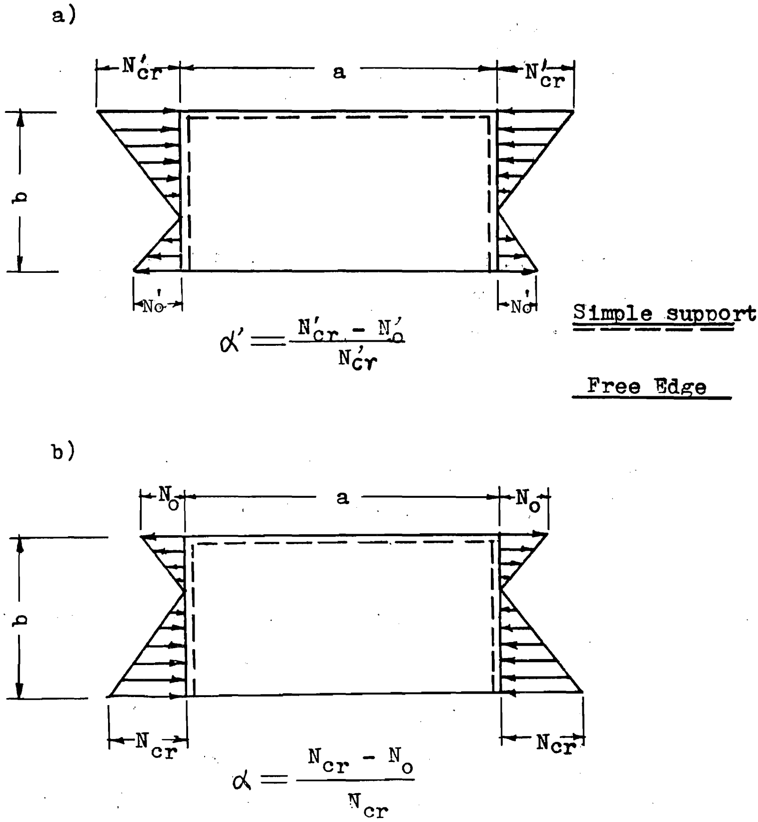


Fig. 1 Plate under Nonuniformly Distributed Compression

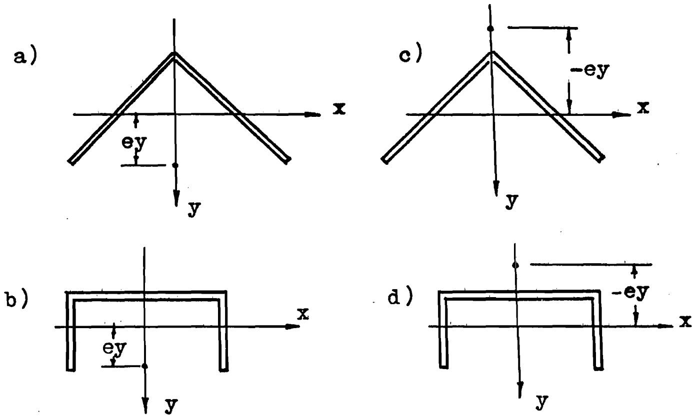


a) and b) Positive Eccentricity of Load

c) and d) Negative Eccentricity of Load

Fig. 2 Definition of Positive and Negative Eccentricity of Load

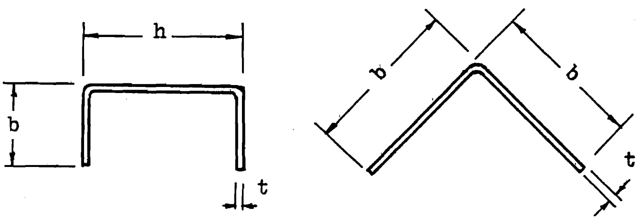


Fig. 3 Cross-section of Specimens

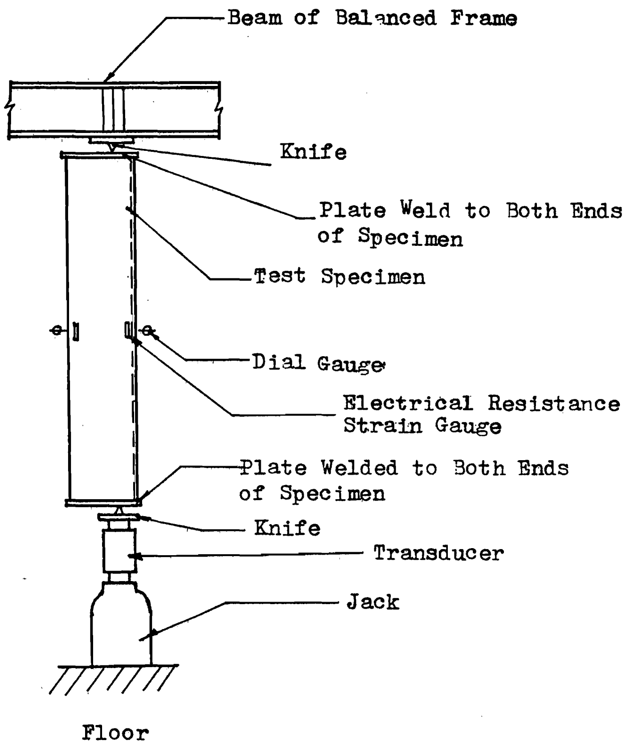


Fig. 4 Experimental Setup and Instrumentation for Specimens

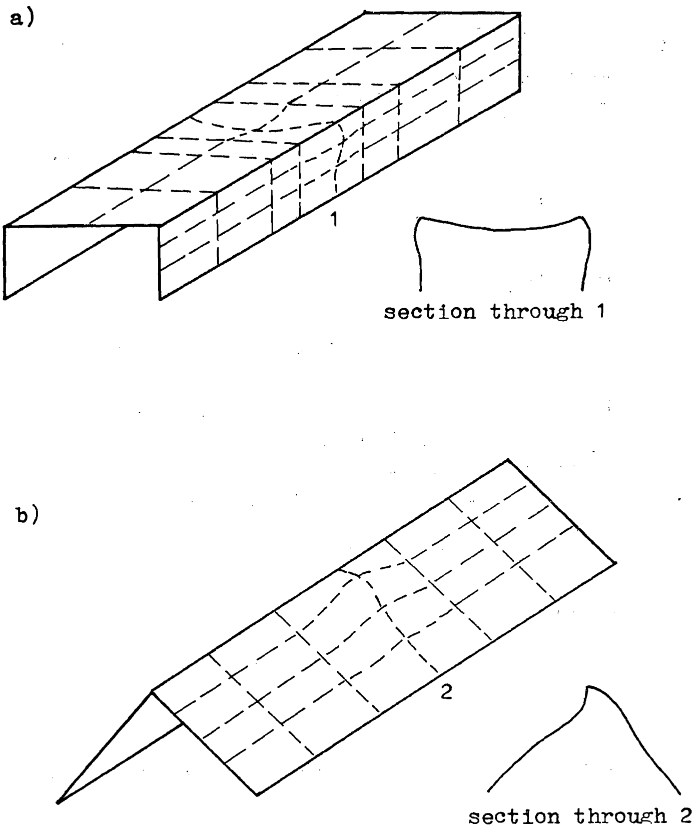


Fig. 5 Buckling Configuration of Specimen